Atomic-scale observation of native oxides on *c*- and *m*-faced GaN surfaces

Jun Uzuhashi[1, *], Yoshihiro Irokawa[1], Toshihide Nabatame[1], Yasuo Koide[1, 2], and Tadakatsu Ohkubo[1]

[1] National Institute for Materials Science, Tsukuba, 305-0047, Japan

[2] Meijo University, Nagoya, Aichi, 468-8502, Japan

* Corresponding author (E-mail: UZUHASHI.Jun@nims.go.jp)

Abstract

Controlling the dielectric/semiconductor interfaces is essential for the development of semiconductor power devices. Gallium nitride (GaN) has attracted significant attention as a next-generation semiconductor owing to its superior properties; however, controlling the dielectric/GaN interface remains a critical challenge unlike silicon (Si). In this study, we observed native oxides formed on both the *c*-face and *m*-face GaN surfaces after simple air exposure using scanning transmission electron microscopy. Oxygen diffusion into Si crystal was significantly suppressed by the formation of a SiO_x layer; on the other hand, gradual oxygen diffusion (Ga-N-O layer) with ~ 2.0 nm depths into the GaN crystal was observed. Remarkably, 1.5 times larger amount oxygen was incorporated in the *m*-face than in the *c*-face GaN. These findings provide key insights into the control of dielectric/GaN interfaces and may facilitate the development of GaN-based power devices.

Gallium nitride (GaN) has attracted significant attention as a material for next-generation power devices because of its excellent properties.[1–6] Metal–oxide–semiconductor field-effect transistors (MOSFETs) are key components in realizing GaN-based power devices, and consequently, considerable research has focused on the properties of dielectric/GaN interfaces since the 1990s.[3,7–35] Structural analyses have revealed that the intermediate GaO_x layer at these interfaces is crystalline rather than amorphous.[8,10,11,19,21,25,28,29,34,35] In contrast to Si—whose oxide consists of a 1–3-nm-thick amorphous SiO_x layer[36-41]—various types of oxides have been reported for GaN, depending on oxidation conditions, which hinder the standardization of GaN surface cleaning processes. [8,10,11,18,19,21,25,28,29,34,35,42,43] Previous reports by mainly employing X-ray diffraction (XRD), transmission electron microscopy (TEM) and X-ray photoelectron spectroscopy (XPS) techniques are as follows; the formations of monoclinic β-Ga_2O_3 phase under the oxidation at 700–950 °C,[8,10,21] or 1.5–3.0 nm-thick $Ga_{(x+2)}N_{3x}O_{(3-3x)}$ compound under dry oxidation at 800 °C for 1 h.[11] Some other types of oxides such as either ε-Ga_2O_3, γ-Ga_2O_3 (111), or their mixture with 1.1–3.5 nm-thicknesses,[25,28] or ~ 2 nm-thick Ga-N-O layer (oxygen gradual diffusion)[34] at the dielectric/GaN interfaces were also reported. In addition to the dielectric/GaN interface, studies have shown that when GaN is exposed to air, a native oxide layer forms, characterized by less than 2 nm GaO_x,[18] or a polarity-inverted Ga-O arrangement similar to bulk β-Ga_2O_3.[42,43] Wolfgang Pauli is credited with saying, "God made the bulk; surfaces were invented by the devil," highlighting surface complexity. In the semiconductor industry, "the surface of Si was gifted by God for humanity" is prevalent because Si surfaces naturally form stable SiO_x layer with outstanding insulating properties. To advance GaN-based devices, clarifying atomic-scale structures of native oxides on GaN surfaces is essential. Since the performance of analytical TEM equipment has improved dramatically in recent years, both *c*- and *m*-face GaN exposed to air were analyzed using aberration-corrected scanning transmission electron microscopy (STEM) combined with energy-dispersive X-ray spectroscopy (EDS).

The *c*- and *m*-face GaN wafers were sequentially cleaned with an acetone, 2-propanol, and H_2SO_4–H_2O_2 mixture, then immersed in buffered hydrofluoric acid for 20 min, and finally rinsed with ultrapure water for 30 s. After the chemical treatment, the wafers were exposed to an air of ~ 25 °C and ~ 20% humidity for 72 h. Subsequently, Ni cap was sputtered to maintain surface conditions. To ensure quality comparisons of STEM-EDS results, cross-sectional STEM lamellae were prepared with 25-nm-thickness using FIB-SEM dual-beam Helios5UX (Thermo Fisher Scientific).[44,45] Atomic-scale high-angle annular dark-field (HAADF-)

and bright-field (BF-) STEM analysis with EDS was performed at 200 kV using a Spectra Ultra S/TEM (Thermo Fisher Scientific). The STEM-EDS data were analyzed using Velox 3.15 program (Thermo Fisher Scientific). For comparison with natural oxide on Si surface, low boron-doped *p*-type (100) Si surface unpacked from carrier and exposed to air at room temperature for half a year was observed. As described below, the abruptness of the atomic structure between the native oxides of Si and GaN cases will be analyzed by comparison using STEM-EDS observations.

An amorphous SiO_x native oxide with a thickness of a few nanometers on a Si surface is shown **in Fig. 1**. **Fig. 1(a)** presents a BF-STEM image of the native oxide on Si, and the EDS compositional profile reveals that the native oxide is SiO_x (**Fig. 1(b)**), as previously reported.[36,39–41] The magnified HAADF-STEM image and the corresponding EDS map, indicated by the rectangle in **Fig. 1(a)**, are shown in **Fig. 1(c,d)**. The EDS map clearly shows that the formation of stable SiO_x strongly prevents the diffusion of oxygen into the Si crystal. A detailed compositional profile is shown later in comparison with GaN (**Fig. 4**).

Fig. 2 shows a *c*-face GaN surface exposed to air. As shown in **Fig. 2(b,c)**, oxygen diffusion (~ 2.0 nm from the *c*-face GaN surface was confirmed by STEM-EDS. **In Fig. 2(c)**, the Ga atomic plane observed at the outermost surface is defined as "1" for the sake of convenience in explanation. The native oxide adhered to both sides of the thin lamellae during the transfer from FIB-SEM to TEM, leading to an overestimation of ~10 at% oxygen. It should be noted that the oxygen composition error bars in **Fig. 2(c)** were estimated by the EDS analysis program used in this study. The atomic-scale EDS maps did not reveal sites occupied by oxygen atoms. Conversely, this suggests that most oxygen atoms likely diffused into interstitial sites rather than forming a specific Ga-O crystal structure; however, some of the N sites may be substituted with oxygen atoms, considering previous XPS studies.[46-48] These XPS studies compared the surface electronic states of GaN grown in vacuum, followed by with/without air exposure. These results suggest that when the GaN surface is exposed to air, the Fermi level shifts toward the conduction band, indicating that oxygen may substitute for N sites within the GaN and act as a donor. While we cannot make definitive statements based solely on EDS maps and estimated error bars, considering previous XPS reports[46–48]—some oxygen may substitute with N sites because both O and N concentrations become high (*i.e.* atomic planes of Ga between 1—2, 2—3, and 3—4).

For designing a GaN-based device, the oxidation state on the *m*-face is also an important insight; thus, the results for *m*-face GaN are shown in **Fig. 3**. To the best of our knowledge, native oxides on *m*-face GaN have not yet been reported. Oxygen diffusion from the *m*-face GaN surface was also confirmed, as in the case of the *c*-face GaN. It is crucial that STEM lamellae are of identical quality when performing comparisons using STEM-EDS. As already mentioned in the method, but worth reiterating due to its importance; we have previously reported methods for controlling the thickness of STEM lamellae and investigated FIB-damage introduced to GaN. [44,45] Based on these techniques and findings, STEM-EDS results comparison was conducted using STEM lamellae guaranteed to be of identical quality. Furthermore, both STEM lamellae were observed under identical conditions within the same TEM session. Therefore, the quality of the STEM lamellae and STEM-EDS analysis condition for *c*- and *m*-faced GaN was guaranteed to be equivalent.

Fig. 4 compares the oxygen compositional changes. In subsequent comparisons, the oxygen background levels were subtracted. While the oxygen in Si drops to background levels within ~ 0.5 ~ nm, the oxygen in both *c*- and *m*-face GaN decreases gradually to ~2.0 nm. This comparison shows that while Si inhibits further oxygen diffusion by forming a stable amorphous oxide layer, oxygen diffusion progresses on the GaN surface exposed to air at room temperature. This oxygen diffusion may be similar to the previous study which reported 1.5–3.0-nm-thick $Ga_{(x+2)}N_{3x}O_{(3-3x)}$.[11] Remarkably, the oxygen composition of *m*-face GaN was ~1.5 times higher than that of *c*-face GaN. This difference is significant even considering the values of the error bars. Although the data are not shown here, similar trends in the oxygen composition on the *c*- and *m*-face surfaces were confirmed in other observation regions as well. It's still within speculation, but this significant difference could be due to the difference in the surface atomic density between the *c*- and *m*-face of GaN crystal structure. If only Ga atoms are considered, the *c*-face is the most densely packed plane (1.136×10^{15} atoms/cm^2), whereas the *m*-face has each atom being more widely spaced (0.605×10^{15} atoms/cm^2).[49] The *m*-face is thought to more readily incorporate oxygen atoms, leading to differences in the oxygen composition between the *c*- and *m*-face GaN surfaces. Finally, we would like to discuss how the state of native oxides changes over time, referencing previous studies. According to previous papers on Si, all studies consistently report a 1–3 nm-thick SiO_x layer. [36–41] While XPS study on the time-dependent changes of SiO_x thickness tended to underestimate it compared to other reports using TEM investigations, it indicated that the thickness of SiO_x reaches saturation after ~7 days. [38] For GaN as well, while prior studies have reported

results under various oxidation conditions, the majority report values between 1.1–3.5 nm. [8,10,11,18,19,21,25,28,29,34,35,42,43] Therefore, the value of ~ 2 nm reported in this paper after 72 h of air exposure falls within these range. While oxidation may slightly progress with continued air exposure, it is unlikely that a drastic change in the native oxide will occur without any other stronger oxidization conditions. Systematically observing the time-dependent changes in native oxide remains another challenge; and the crucial issue in this study is that oxygen diffuses to a depth of ~ 2 nm in GaN bulk simply through air exposure.

In summary, this study clarified the native oxides on both *c*- and *m*-face GaN after air exposure for 72 h at room temperature. Atomic resolution STEM-EDS analysis revealed no specific crystal structure but indicated that oxygen diffuses ~ 2.0 nm (Ga-N-O layer) from the surface into GaN, and some of the O atoms may substitute N sites. Under the same observation conditions, no oxygen diffusion is observed for Si. However, unlike Si, previous studies have suggested that the formation of native oxides on GaN may vary depending on the oxidation conditions. A comparison of the *c*- and *m*-face GaN revealed that more than 1.5 times larger amount of oxygen incorporated into the *m*-face GaN.

Supplementary Material

Supplementary Material shows annular bright-field (ABF-) STEM images and EDS compositional profile of the native oxide on *c*-face GaN with annealing at 200 °C for 2 h with epoxy resin cap (one of the materials widely used as the cap on the surface in TEM lamellae preparation procedure) to cure it. Even after relatively low-temperature annealing, different types of native oxide structures were formed. This suggests that, unlike Si, the types of native oxides on the GaN surface are sensitive to the oxidation conditions and that the choice of TEM lamellae preparation method is also crucial for elucidating the native oxide on most surfaces.

Acknowledgments

This research was supported by the Ministry of Education, Culture, Sports, Science and Technology, Japan (MEXT), through its “Creation of Innovative Core Technology for Power Electronics” program under Grant No. JPJ009777, and ARIM (JPMXP1223NM5088). A part of this study was supported by the Electron Microscopy Unit of the National Institute for Materials Science (NIMS). The authors thank Kyoko Suzuki for her technical support.

Conflict of Interest Statement

The authors have no conflicts to disclose.

CRediT Author Contributions

Jun Uzuhashi: Conceptualization, Data Curation, Visualization, Writing, and Original Draft Preparation. **Yoshihiro Irokawa**: Conceptualization, Writing/Review & Editing. **Toshihide Nabatame**: Conceptualization, Writing/Review & Editing. **Yasuo Koide**: Supervision, Writing/Review & Editing. **Tadakatsu Ohkubo**: Supervision, Writing/Review & Editing.

Data Availability Statement

Data will be made available on request.

References

[1]T. P. Chow and R. Tyagi, IEEE Trans. Electron Devices **41**, 1481–1483 (1994). https://doi.org/10.1109/16.297751

[2]S. J. Pearton, J. C. Zolper, R. J. Shul, and F. Ren, J. Appl. Phys. **86**, 1–78 (1999). https://doi.org/10.1063/1.371145

[3]S. J. Pearton, F. Ren, A. P. Zhang, and K. P. Lee, Mater. Sci. Eng. R. Rep. **30**, 55–212 (2000). https://doi.org/10.1016/S0927-796X(00)00028-0

[4]B. J. Baliga, Semicond. Sci. Technol. **28**, 074011 (2013). https://doi.org/10.1088/0268-1242/28/7/074011

[5]T. Kachi, Jpn. J. Appl. Phys. **53**, 100210 (2014). https://doi.org/10.7567/JJAP.53.100210

[6]J. Millan, P. Godignon, X. Perpina, A. Perez-Tomas, and J. Rebollo, IEEE Trans. Power Electron. **29**, 2155–2163 (2014). https://doi.org/10.1109/TPEL.2013.2268900

[7]Jr H. C. Casey, G. G. Fountain, R. G. Alley, B. P. Keller, and S. P. DenBaars, Appl. Phys. Lett. **68**, 1850–1852 (1996). https://doi.org/10.1063/1.116034

[8]S.D. Wolter, S.E. Mohney, H.S. Venugopalan, A.E. Wickenden, D.D. Koleske, J. Electrochem. Soc. 145, 629 (1998). https://doi.org/10.1149/1.1838314

[9]S. J. Pearton, H. Cho, J. R. LaRoche, F. Ren, R. G. Wilson, and J. W. Lee, Appl. Phys. Lett. **75**, 2939–2941 (1999). https://doi.org/10.1063/1.125194

[10]E. D. Readinger, S. D. Wolter, D. L. Waltemyer, J. M. Delucca, S. E. Mohney, B. I. Prenitzer, L. A. Giannuzzi, and R. J. Molnar, J. Electron. Mater. **28**, 257–260 (1999). https://doi.org/10.1007/s11664-999-0024-z

[11]S. D. Wolter, J. M. DeLucca, S. E. Mohney, R. S. Kern, and C. P. Kuo, Thin Solid Films **371**, 153–160 (2000). https://doi.org/10.1016/S0040-6090(00)00984-6

[12]T. Sawada, Y. Ito, K. Imai, K. Suzuki, H. Tomozawa, and S. Sakai, Appl. Surf. Sci. **159–160**, 449–455 (2000). https://doi.org/10.1016/S0169-4332(00)00060-X

[13]R. Therrien, G. Lucovsky, and R. Davis, Appl. Surf. Sci. **166**, 513–519 (2000). https://doi.org/10.1016/S0169-4332(00)00485-2

[14]C. Bae and G. Lucovsky, Surf. Sci. **532–535**, 759–763 (2003). https://doi.org/10.1016/S0039-6028(03)00181-X

[15]T. Hashizume, S. Ootomo, and H. Hasegawa, Appl. Phys. Lett. **83**, 2952–2954 (2003). https://doi.org/10.1063/1.1616648

[16]Y. Nakano, T. Kachi, and T. Jimbo, Appl. Phys. Lett. **83**, 4336–4338 (2003). https://doi.org/10.1063/1.1629371

[17]C. Bae and G. Lucovsky, J. Vac. Sci. Technol. A **22**, 2402–2410 (2004). https://doi.org/10.1116/1.1807396

[18]Y. J. Lin, W. X. Lin, C. T. Lee, and H. C. Chang, Jpn. J. Appl. Phys. **45**, 2505 (2006). https://doi.org/10.1143/JJAP.45.2505

[19]N. Shiozaki, T. Sato, and T. Hashizume, Jpn. J. Appl. Phys. 46 1471 (2007). https://doi.org/10.1143/JJAP.46.1471

[20]Y. Niiyama, T. Shinagawa, S. Ootomo, H. Kambayashi, T. Nomura, and S. Yoshida, Phys. Status Solidi A **204**, 2032–2036 (2007). https://doi.org/10.1002/pssa.200674844

[21]Y. Zhou, C. Ahyi, T. Isaacs-Smith, M. Bozack, C. C. Tin, J. Williams, M. Park, A. J. Cheng, J. H. Park, D. J. Kim, D. Wang, E.A. Preble, A. Hanser, and K. Evans, Solid-State Electron. 52, 756–764 (2008). https://doi.org/10.1016/j.sse.2007.10.045

[22]K. Yamaji, M. Noborio, J. Suda, and T. Kimoto, Jpn. J. Appl. Phys. **47**, 7784 (2008). https://doi.org/10.1143/JJAP.47.7784

[23]B. S. Eller, J. Yang, and R. J. Nemanich, J. Vac. Sci. Technol. A **31**, 050807 (2013). https://doi.org/10.1116/1.4807904

[24]T. Oka, T. Ina, Y. Ueno, and J. Nishii, Appl. Phys. Express **8**, 054101 (2015). https://doi.org/10.7567/APEX.8.054101

[25]Y. Irokawa, T.T. Suzuki, K. Yuge, A. Ohi, T. Nabatame, K. Kimoto, T. Ohnishi, K. Mitsuishi, and Y. Koide, Jpn. J. Appl. Phys. **56**, 128004 (2017). https://doi.org/10.7567/JJAP.56.128004

[26]T. Yamada, J. Ito, R. Asahara, K. Watanabe, M. Nozaki, T. Hosoi, T. Shimura, and H. Watanabe, Appl. Phys. Lett. **110**, 261603 (2017). https://doi.org/10.1063/1.4990689

[27]V. M. Bermudez, Surf. Sci. Rep. **72**, 147–315 (2017). https://doi.org/10.1016/j.surfrep.2017.05.001

[28]K. Mitsuishi, K. Kimoto, Y. Irokawa, T. Suzuki, K. Yuge, T. Nabatame, S. Takashima, K. Ueno, M. Edo, K. Nakagawa, and Y. Koide, Jpn. J. Appl. Phys. **56**, 110312 (2017). https://doi.org/10.7567/JJAP.56.110312

[29]Y. Irokawa, K. Mitsuishi, T. Nabatame, K. Kimoto, and Y. Koide, Jpn. J. Appl. Phys. **57**, 118003 (2018). https://doi.org/10.7567/JJAP.57.098003

[30]T. Yamada, K. Watanabe, M. Nozaki, H. Yamada, T. Takahashi, M. Shimizu, A. Yoshigoe, T. Hosoi, T. Shimura, and H. Watanabe, Appl. Phys. Express **11**, 015701 (2018). https://doi.org/10.7567/APEX.11.015701

[31]M. Hirose, T. Nabatame, K. Yuge, E. Maeda, A. Ohi, N. Ikeda, Y. Irokawa, H. Iwai, H. Yasufuku, S. Kawada, M. Takahashi, K. Ito, Y. Koide, H. Kiyono, Microelectron. Eng. **216**, 111040 (2019). https://doi.org/10.1016/j.mee.2019.111040

[32]Y. Irokawa, T. Nabatame, T. Sawada, M. Miyamoto, H. Miura, K. Tsukagoshi, and Y. Koide, ECS J. Solid State Sci. Technol. **13**, 085003 (2024). https://doi.org/10.1149/2162-8777/ad6fd2

[33]M. Hara, T. Nabatame, T. Sawada, M. Miyamoto, H. Miura, Y. Irokawa, T. Kimoto, and Y. Koide, Mater. Sci. Semicond. Process. **196**, 109606 (2025). https://doi.org/10.1016/j.mssp.2025.109606

[34]J. Uzuhashi, Y. Irokawa, T. Nabatame, T. Ohkubo, and Y. Koide, ECS J. Solid State Sci. Technol. **14**, 085001 (2025). https://doi.org/10.1149/2162-8777/adf3e3

[35]E. Kano, S. Hattori, K. Shiraishi, A. Oshiyama, T. Umeda, T. Narita, T, Kachi, and N. Ikarashi, Appl. Phys. Lett. **127**, 032112 (2025). https://doi.org/10.1063/5.0274521

[36]J.H. Mazur, R. Gronsky, J. Washburn, Chapter of Microscopy of Semiconducting Materials 1983, Third Oxford Conference on Microscopy of Semiconducting Materials, St Catherines College, March 1983 (1983).

https://doi.org/10.1201/9781003069614

[37]P. J. Grunthaner, M. H. Hecht, F. J. Grunthaner, and N. M. Johnson, J. Appl. Phys. **61**, 629–638 (1987). https://doi.org/10.1063/1.338215

[38]M. Morita, T. Ohmi, E. Hasegawa, M. Kawakami, and M. Ohwada, J. Appl. Phys. **68**, 1272–1281 (1990). https://doi.org/10.1063/1.347181

[39]M. J. Kim and R. W. Carpenter, J. Mater. Res. **5**, 347–351 (1990). https://doi.org/10.1557/JMR.1990.0347

[40]A. Chin, B. C. Lin, W. J. Chen, Y. B. Lin, and C. Tsai, IEEE Electron Device Lett. **19**, 426–428 (1998). https://doi.org/10.1109/55.728901

[41]T. Plach, K. Hingerl, S. Tollabimazraehno, G. Hesser, V. Dragoi, and M. Wimplinger, J. Appl. Phys. **113**, 094905 (2013). https://doi.org/10.1063/1.4794319

[42]J. H. Dycus, K. J. Mirrielees, E. D. Grimley, R. Kirste, S. Mita, Z. Sitar, R. Collazo, D. L. Irving, and J. M. LeBeau, ACS Appl. Mater. Interfaces **10**, 10607–10611 (2018). https://doi.org/10.1021/acsami.8b00845

[43]K. J. Mirrielees, J. H. Dycus, J. N. Baker, P. Reddy, R. Collazo, Z. Sitar, J.M. LeBeau, and D. L. Irving, J. Appl. Phys. **129**, 195304 (2021). https://doi.org/10.1063/5.0048820

[44]J. Uzuhashi and T. Ohkubo, Ultramicroscopy **262**, 113980 (2024). https://doi.org/10.1016/j.ultramic.2024.113980

[45]J. Uzuhashi, Y. Yao, T. Ohkubo, and T. Sekiguchi, Microscopy **74**, 279-285 (2025). https://doi.org/10.1093/jmicro/dfaf006

[46]M. Kočan, A. Rizzi, H. Lüth, S. Keller, and U. K. Mishra, Phys. Stat. Sol. (B) **234**, 773–777 (2002). https://doi.org/10.1002/1521-3951(200212)234:3%3C773::AID-PSSB773%3E3.0.CO;2-0

[47]Y. Dong, R. M. Feenstra, and J. E. Northrup, J. Vac. Sci. Technol. B **24**, 2080–2086 (2006). https://doi.org/10.1116/1.2214713

[48]D. Majchrzak, M. Grodzicki, P. Ciechanowicz, J. Rousset, D. E.dyta Piskorska-Hommel, and D. Hommel, Acta Phys. Pol. A **136**, 585–588 (2019). http://doi.org/10.12693/APhysPolA.136.585

[49]C. B. Lim, A. Ajay, and E. Monroy, Appl. Phys. Lett. **111**, 022101 (2017). https://doi.org/10.1063/1.4993570

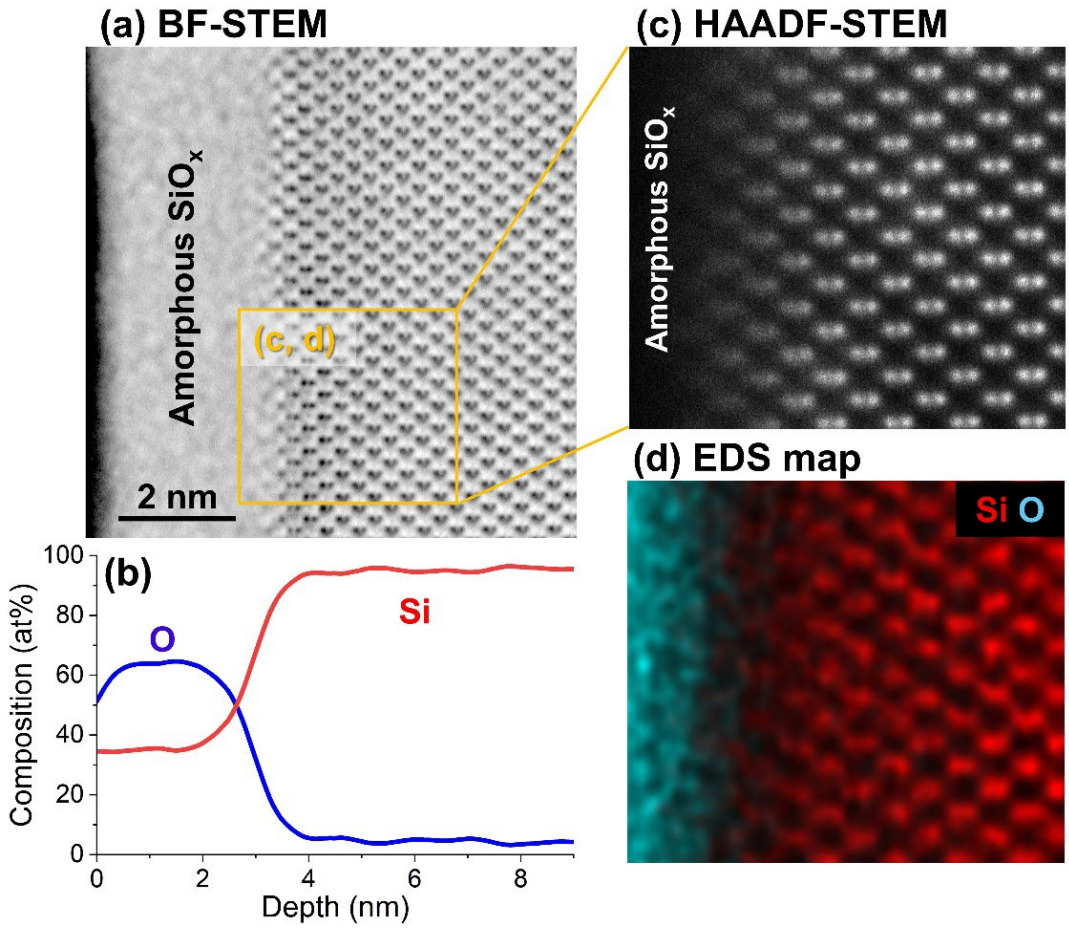

Figure 1. (a) Cross-sectional BF-STEM image of amorphous SiO_x layer formed on the *p*-Si (100) surface, and (b) corresponding EDS compositional profile from the amorphous SiO_x layer to Si crystal. (c,d) Higher-magnification HAADF-STEM image and EDS elemental map of SiO_x/Si interface indicated in (a).

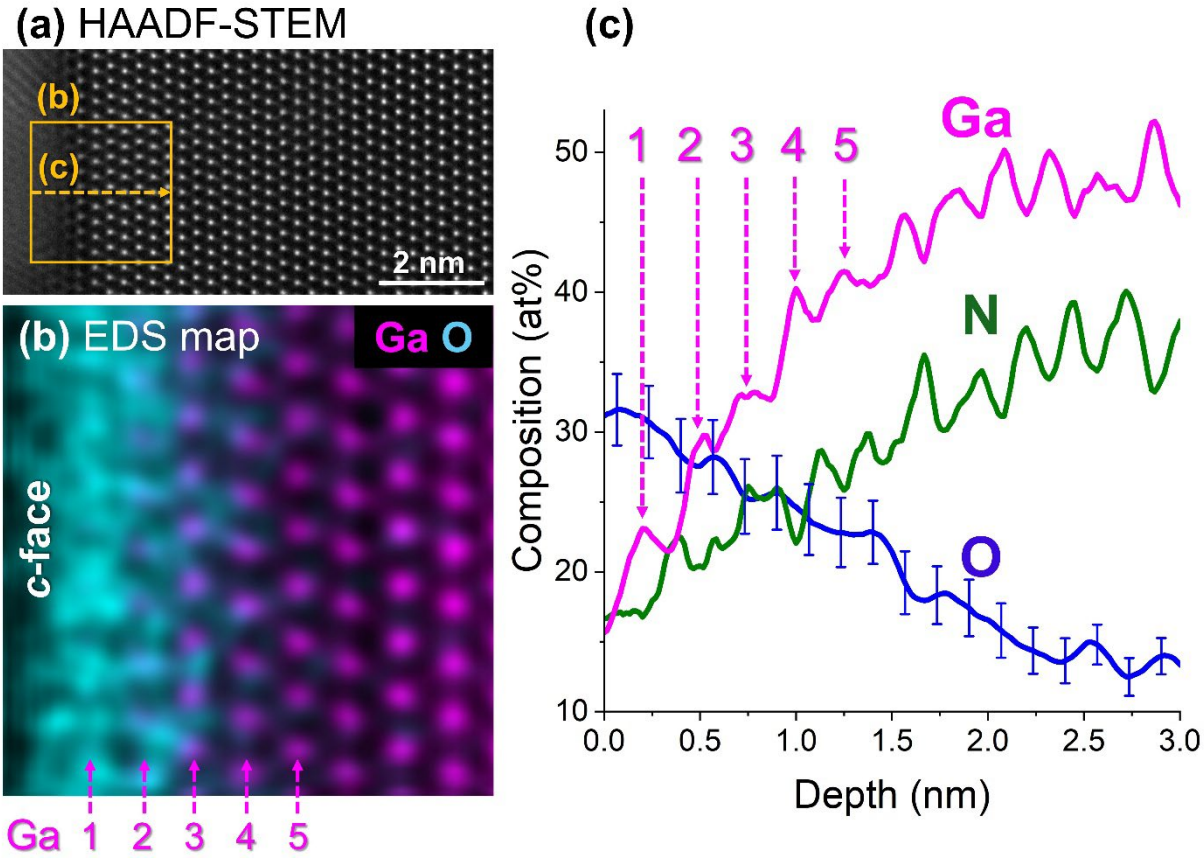

Figure 2. (a) Cross-sectional HAADF-STEM image of *c*-face GaN surface with air exposure at room temperature for 72 h. (b) EDS elemental map, and (c) EDS compositional profile from the surface into the bulk.

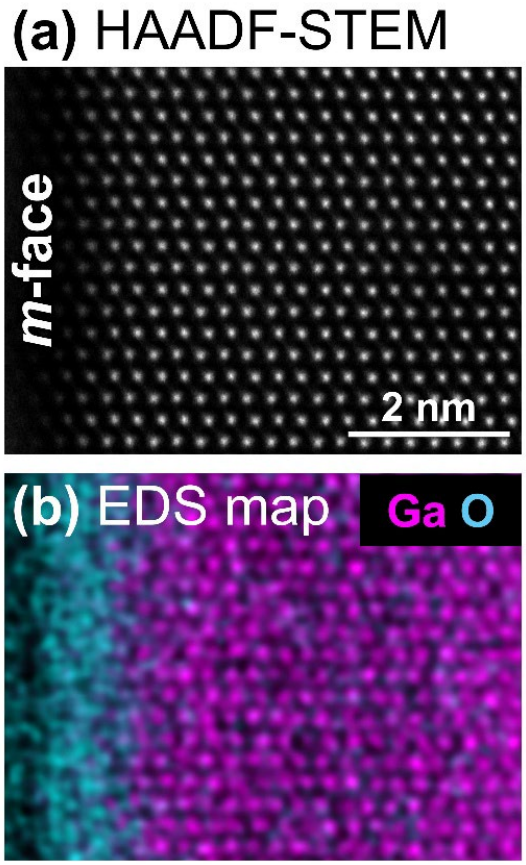

Figure 3. (a) Cross-sectional HAADF-STEM image of *m*-face GaN surface. (b) EDS elemental map from the same field of view as HAADF-STEM image.

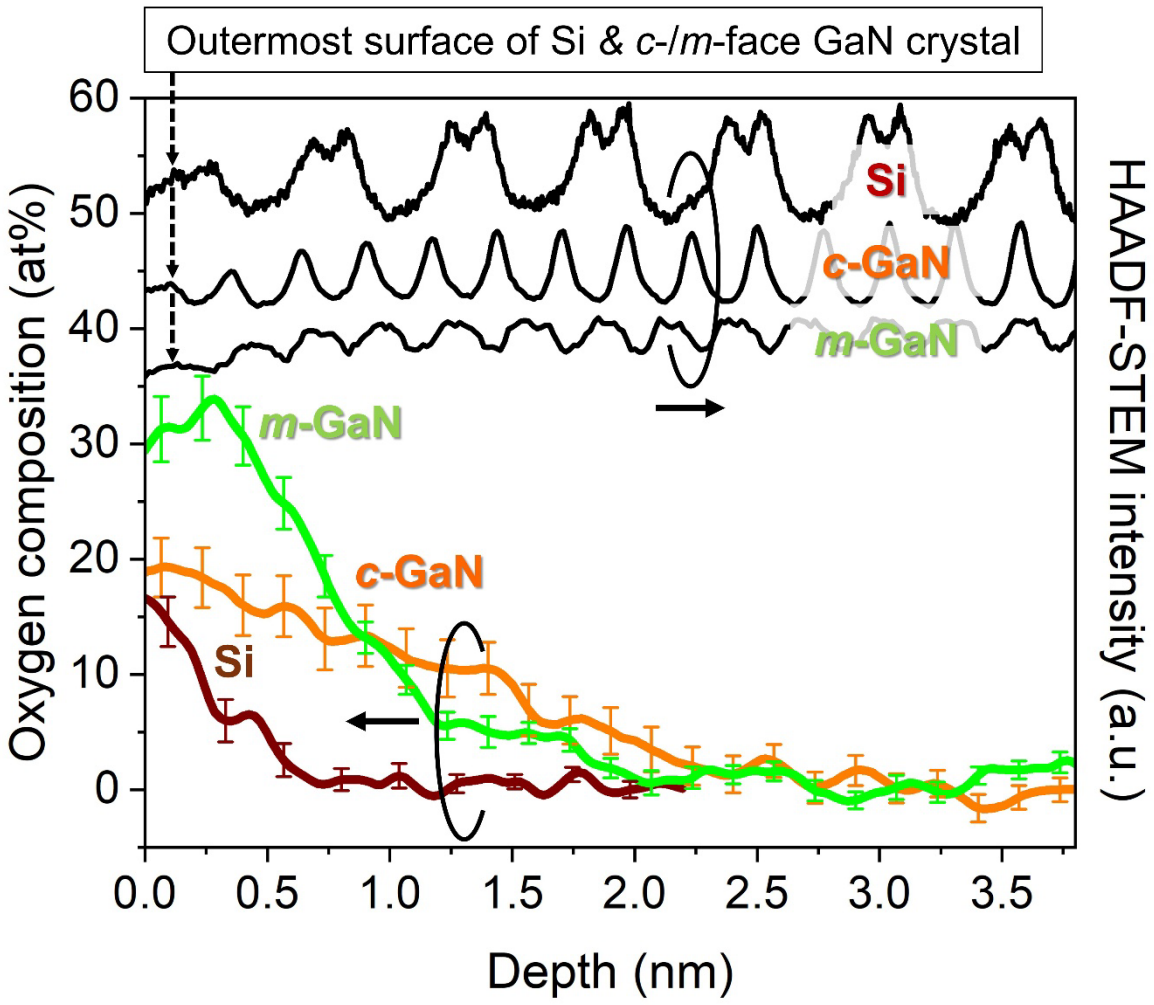

Figure 4. Comparison of oxygen compositional changes on Si, *c*- and *m*-face GaN surfaces by defining the position of the topmost Ga or Si atomic plane as the surface. The depth of 0.1 nm in the graph corresponds to the surface. To ensure a fair comparison, the oxygen values (at%) were plotted after subtracting the background oxygen level at a sufficiently deep position (11.2 at% for Si, 12.3 at% for *c*-face GaN, and 8.1 at% for *m*-face GaN).

Supplementary Material

Annular bright-field (ABF-) STEM images and EDS compositional profile of the native oxide on *c*-face GaN with epoxy resin cap (one of the materials widely used as the cap on the surface in TEM lamellae preparation procedure) followed by annealing at 200 °C for 2 h to cure it. Even after relatively low-temperature annealing, different types of native oxide structures were formed. The outermost few atomic layers differ from the wurtzite structure of GaN, rather similar to β-Ga_2O_3.